HAL
open science

Simple model of a coherent molecular photocell

Matthias Ernzerhof, Marc-André Bélanger, Didier Mayou, Tahereh Nematiaram

To cite this version:

Matthias Ernzerhof, Marc-André Bélanger, Didier Mayou, Tahereh Nematiaram. Simple model of a coherent molecular photocell. The Journal of Chemical Physics, 2016, 144 (13), pp.134102 - 164326. 10.1063/1.4944468 . hal-01620569

HAL Id: hal-01620569

https://hal.science/hal-01620569v1

Submitted on 20 Oct 2017

HAL is a multi-disciplinary open access archive for the deposit and dissemination of scientific research documents, whether they are published or not. The documents may come from teaching and research institutions in France or abroad, or from public or private research centers.

L'archive ouverte pluridisciplinaire **HAL**, est destinée au dépôt et à la diffusion de documents scientifiques de niveau recherche, publiés ou non, émanant des établissements d'enseignement et de recherche français ou étrangers, des laboratoires publics ou privés.

AIP | The Journal of Chemical Physics

Simple model of a coherent molecular photocell

Matthias Ernzerhof, Marc-André Bélanger, Didier Mayou, and Tahereh Nemati Aram

Citation: The Journal of Chemical Physics **144**, 134102 (2016); doi: 10.1063/1.4944468
View online: http://dx.doi.org/10.1063/1.4944468
View Table of Contents: http://scitation.aip.org/content/aip/journal/jcp/144/13?ver=pdfcov
Published by the AIP Publishing

Articles you may be interested in

Coherent destruction of tunneling in a six-dimensional model of NHD2: A computational study using the multi-configuration time-dependent Hartree method
J. Chem. Phys. **141**, 164326 (2014); 10.1063/1.4900518

Coherent and incoherent contributions to the carrier-envelope phase control of wave packet localization in quantum double wells
J. Chem. Phys. **140**, 184316 (2014); 10.1063/1.4874876

A simple model of molecular electronic devices and its analytical solution
J. Chem. Phys. **127**, 204709 (2007); 10.1063/1.2804867

Measurement of the electronic transition dipole moment by Autler-Townes splitting: Comparison of three- and four-level excitation schemes for the Na 2 A Σ u + 1 − X Σ g + 1 system
J. Chem. Phys. **124**, 084308 (2006); 10.1063/1.2164454

Experimental study of the NaK 3 Π 3 double minimum state
J. Chem. Phys. **122**, 144313 (2005); 10.1063/1.1875132

Reuse of AIP Publishing content is subject to the terms: https://publishing.aip.org/authors/rights-and-permissions. Downloaded to IP: 147.173.66.125 On: Fri, 06 May 2016 07:53:59

THE JOURNAL OF CHEMICAL PHYSICS **144**, 134102 (2016)

Simple model of a coherent molecular photocell

Matthias Ernzerhof,[1,a)] Marc-André Bélanger,[1] Didier Mayou,[2] and Tahereh Nemati Aram[2]
[1]*Département de Chimie, Université de Montréal, C.P. 6128 Succursale A, Montréal, Québec H3C 3J7, Canada*
[2]*Institut Néel, CNRS, F-38042 Grenoble, France*

(Received 1 November 2015; accepted 7 March 2016; published online 1 April 2016)

Electron transport in molecular electronic devices is often dominated by a coherent mechanism in which the wave function extends from the left contact over the molecule to the right contact. If the device is exposed to light, photon absorption in the molecule might occur, turning the device into a molecular photocell. The photon absorption promotes an electron to higher energy levels and thus modifies the electron transmission probability through the device. A model for such a molecular photocell is presented that minimizes the complexity of the problem while providing a non-trivial description of the device mechanism. In particular, the role of the molecule in the photocell is investigated. It is described within the Hückel method and the source-sink potential approach [F. Goyer, M. Ernzerhof, and M. Zhuang, J. Chem. Phys. **126**, 144104 (2007)] is used to eliminate the contacts in favor of complex-valued potentials. Furthermore, the photons are explicitly incorporated into the model through a second-quantized field. This facilitates the description of the photon absorption process with a stationary state calculation, where eigenvalues and eigenvectors are determined. The model developed is applied to various generic molecular photocells. © *2016 AIP Publishing LLC*. [http://dx.doi.org/10.1063/1.4944468]

I. INTRODUCTION

Photovoltaic devices constructed from molecules attached to semiconductor surfaces are a focus of intense research (for a review see, e.g., Ref. 1). A little explored variant[2–5] of photovoltaic cells is derived from single molecules (Fig. 1) and exhibits a predominantly coherent mechanism. This mechanism is characterized by a wave function that extends over the entire device and that determines its properties. It has to be contrasted to the mechanism of a conventional dye sensitized solar cell which typically involves a sequence of steps that occur in a de-coherent manner. In a de-coherent mechanism, the electron transfer from the electrolyte to the molecule, for instance, is in general not described by a wave function that also accounts for the transfer of the excited electron to the conduction band of the semi-conductor. In the theories of Grätzel cells and in other examples for the interaction between light and matter, the electromagnetic field is usually considered in a semi-classical manner through the addition of suitable time-dependent vector and scalar potentials to the molecular Hamiltonian.[6,7] Coherently controlled molecular junctions, very similar to the systems considered here, have been studied in detail by Peskin, Galperin, and co-workers.[8–12] Also in these examples, the field is described in the conventional semi-classical manner. We adopt an alternative approach that is less frequently employed[2–5] and in which the electromagnetic field is quantized and then coupled to the system consisting of the molecule and the contacts. While this appears to be more involved than the semiclassical variant, it enables us to describe the photon absorption as a stationary process, avoiding a time-dependent approach. An eigenvalue equation is solved instead with a suitable model Hamiltonian whose construction we describe in detail. The quantized-field model simplifies the description of the photocell from a conceptual as well as computational perspective. These advantages provide the motivation for the development of the model rather than a need for a quantized description. In typical photovoltaic devices, the number of photons is infinite and there is no reason to believe that a semiclassical approach would fail. On the other hand, considering elementary processes involving states of well-defined photon numbers is, of course, not wrong and it reveals the fundamental steps.

In the most basic example discussed below, the photon absorption is modeled as a superposition of two wave functions, one in which the molecule is in its ground state and where the system contains n photons, and a second one where the molecule is in an excited state with $n-1$ photons. These two states are coupled to each other through the electric field generated by the photons. Furthermore, the system consisting of the molecule and photons is coupled to a left and a right macroscopic contact (Fig. 1). Therefore, a photon induced current can arise. To account for the interaction of the molecule with the contacts, we rely on the source-sink potential (SSP) method,[13–15] which has been developed to describe molecular electronic devices.[16] As with the SSP method, the model proposed here does not aim at a quantitative description of the complicated steady state of a molecular photocell, rather we want to provide a minimalistic, paper and pencil description.

While coherent molecular photocells have not yet been systematically investigated, their realization appears to be

a)Author to whom correspondence should be addressed. Electronic mail: Matthias.Ernzerhof@UMontreal.ca

 © 2016 AIP Publishing LLC

Reuse of AIP Publishing content is subject to the terms: https://publishing.aip.org/authors/rights-and-permissions. Downloaded to IP: 147.173.66.125 On: Fri, 06 May 2016 07:53:59

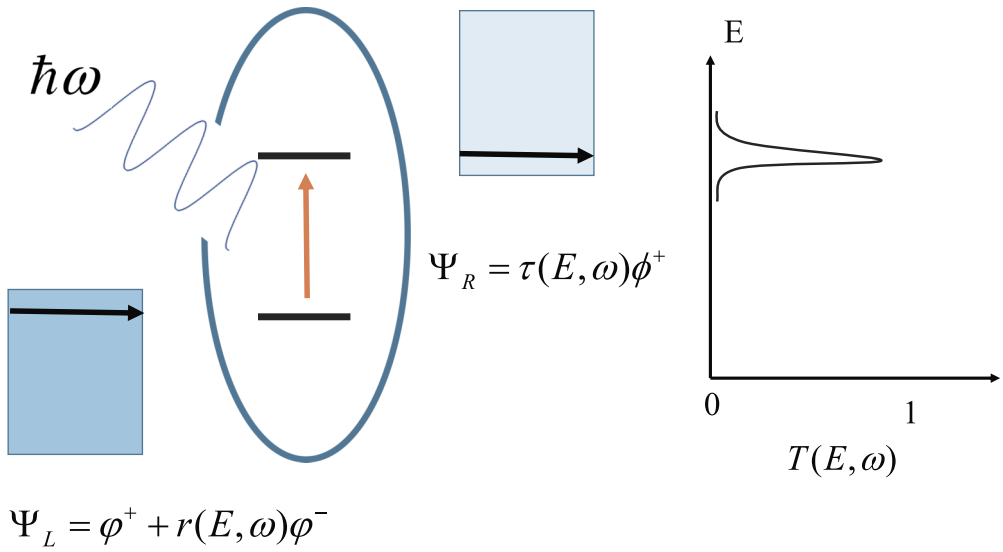

FIG. 1. Schematic representation of a coherent molecular photovoltaic cell. A very basic cell is chosen that reduces the requirements on the corresponding model to a minimum while still retaining the essential elements of a coherent molecular photocell. The left (L) contact has only a valence band in the range of energies relevant for the simple photocell. Similarly, on the right (R), the molecule couples to the conduction band exclusively. To obtain a current through the device, a photon has to be absorbed. At a given total energy E, the incoming electron wave (φ^+) of energy $E-\omega$ ($\hbar = 1$ in atomic units) is partially reflected (φ^-) in the left contact. The corresponding reflection coefficient is $r(E,\omega)$. In the right contact, the outgoing electron wave (ϕ^+) is multiplied by the transmission amplitude $\tau(E,\omega)$, where the energy of the outgoing wave is now increased by the photon energy ω to a value given by E. On the right, a sketch of the transmission probability $T(E,\omega) = 1-|r(E,\omega)|^2$ is shown with a maximum at the LUMO energy.

within the reach of modern experimental techniques.[17] In typical experiments on molecular junctions, some of the coherent processes considered in our model might be blurred due to coupling to external baths and due to averaging over a range of photon and electron energies. However, we would expect that experimental setups can be developed that preserve the simple coherent mechanism described here. This optimism is supported by theory and experiments (e.g., Refs. 13 and 18–22) on molecular junctions in which interference effects, relying on coherent device wave functions, often dominate the device mechanism. Our model requires an extension of these interference effects to systems that interact with external light sources. As demonstrated in the area of coherent control theory,[23] there are sophisticated experimental techniques that enable a coherent interaction of light with molecules. On the other hand, following the examples of Refs. 10 and 24, it might also be possible to include decoherence effects in the model developed here.

Finally we note that the photons in our theory can be replaced by other quasi-particles such as phonons. The corresponding model of electrons coupled to a quantized phonon field has been developed in and applied to molecular junctions.[25]

In Section II, we develop a model for the photocell and in Section III, we provide various illustrations for our model.

II. DESIGN OF A MODEL FOR A COHERENT MOLECULAR PHOTOCELL

The photocell (Fig. 1) can be subdivided into the left contact (L), the molecule (M), and the right contact (R). In addition, the photons have to be incorporated into the model as well as the interactions between the four subsystems. We address the subsystems one by one, starting with the electrons in the molecule, and explain how to model them. Furthermore, we discuss the coupling between the subsystems. We use atomic units ($\hbar = e^2 = m_e = 1$) throughout the article.

A. Electrons

To describe the electronic structure of the molecule, we employ the Hückel approximation in which solely the π-electron system created by the sp^2 carbon atoms is accounted for. Only nearest neighbor interactions are considered and the coupling matrix element is denoted by t. The zero-energy reference value can be chosen freely and we shift the diagonal matrix elements of the Hückel Hamiltonian to zero. To facilitate the description of the coupling between photons and electrons, we do not employ the Hückel matrix Hamiltonian directly, but represent it on the basis of the molecular orbitals $\{\varphi_i\}_{i=1,\ldots,N}$ that are obtained as eigenfunctions of the Hückel Hamiltonian. In a second quantized representation, the electronic Hamiltonian H_{el} is given by

$$H_{\mathrm{el}} = \sum_i \epsilon_i b_i^\dagger b_i. \tag{1}$$

In this Hamiltonian, the electron orbitals φ_i are associated with creation and annihilation operators denoted by $b_i^\dagger$ and b_i, respectively.

The Hückel model has, of course, its limitations with regard to the diversity of systems and phenomena that it can describe. However, a past experience (see, e.g., Refs. 19 and 26) shows that it is surprisingly useful for a qualitative description and often it suffices to explain key physical properties.

Reuse of AIP Publishing content is subject to the terms: https://publishing.aip.org/authors/rights-and-permissions. Downloaded to IP: 147.173.66.125 On: Fri, 06 May 2016 07:53:59

B. Photons

Following the presentation of Ref. 27, the electromagnetic field is accounted for as a quantized field. Before switching to a matrix representation which is used to perform the actual calculations, the Hamiltonian of the photons $H_{\rm ph}$ is most conveniently written in second quantized form

$$H_{\rm ph} = \sum_{\vec{v}} \int d^3k\ \omega_{\vec{k}} a^{\dagger}_{\vec{k},\vec{v}} a_{\vec{k},\vec{v}}, \tag{2}$$

where $\vec{v}$ is a unit vector characterizing the photon polarization, $\vec{k}$ is the photon wave vector, and $\omega_{\vec{k}} = kc$, where c is the speed of light. $a^{\dagger}_{\vec{k},\vec{v}}$ and $a_{\vec{k},\vec{v}}$ are photon creation and annihilation operators, respectively.

The photons are then coupled to the electronic degrees of freedom through the introduction of the quantized vector potential $\vec{A}(\vec{r})$ of the form

$$\vec{A}(\vec{r}) = \sum_{\vec{v}} \vec{v} \int d^3k \sqrt{\frac{1}{16\pi^3\varepsilon_0\omega_{\vec{k}}}} \left(e^{-\mathrm{i}\vec{k}\cdot\vec{r}} a^{\dagger}_{\vec{k},\vec{v}} + e^{\mathrm{i}\vec{k}\cdot\vec{r}} a_{\vec{k},\vec{v}}\right), \tag{3}$$

where ε_0 is the vacuum permittivity. Before the operator in Eq. (3) is combined with the electronic Hamiltonian, we perform various simplifications. First, we use the well known fact that the product $\vec{k}\cdot\vec{r}$ is very small in the context of the molecular systems considered. The product $\vec{k}\cdot\vec{r}$ indicates the variation of the photon wavelength on the molecular scale. The molecular size is in the range of Ångströms and the photon wavelength is on the order of thousands of Ångströms. Therefore the exponents $e^{\mathrm{i}\vec{k}\cdot\vec{r}}$ in Eq. (3) can be replaced by 1, which corresponds to the well known dipole approximation. Furthermore, to couple $\vec{A}$ to the electronic degrees of freedom, we employ the conventional substitution $\vec{p} \to \vec{p} - \vec{A}$. Then since $\vec{A}$ is assumed to be negligible in relation to $\vec{p}$, $(\vec{p} - \vec{A})^2 \approx \vec{p}^2 - \vec{A}\cdot\vec{p}$. Here we employ the Coulomb gauge for $\vec{A}$ so that $\vec{p}\cdot\vec{A} = 0$. With these assumptions, the coupling of the vector potential to the electronic Hamiltonian results in an additive term in the Hamiltonian of the form

$$V = \sum_{\vec{v}} \int d^3k\ \ C(\vec{k}) \left(a^{\dagger}_{\vec{k},\vec{v}} + a_{\vec{k},\vec{v}}\right) \vec{p}\cdot\vec{v}, \tag{4}$$

where $C(\vec{k}) = \sqrt{\frac{1}{16\pi^3\varepsilon_0\omega_{\vec{k}}}}$. In Eq. (4), the vector describing the photon polarization ($\vec{v}$) multiplies the electron momentum operator $\vec{p}$. To couple the photons to the electrons, we combine Eqs. (1), (2), and (4). The electronic degrees of freedom appear in Eq. (4) through the electron momentum operator $\vec{p}$ that we expressed in second-quantized form

$$H_{\rm el,ph} = \sum_i \epsilon_i b^{\dagger}_i b_i + \sum_{\vec{v}} \int d^3k\ \omega_{\vec{k}} a^{\dagger}_{\vec{k},\vec{v}} a_{\vec{k},\vec{v}} + \sum_{i,j,\vec{v}} \int d^3k\ C(\vec{k}) \vec{v}\cdot\vec{p}_{ij} b^{\dagger}_i b_j \left(a^{\dagger}_{\vec{k},\vec{v}} + a_{\vec{k},\vec{v}}\right). \tag{5}$$

The momentum operator appearing in this expression is inconvenient. To replace it by the position operator, one uses the well known commutator relation

$$\mathrm{i}\vec{p} = [\vec{r}, H]. \tag{6}$$

Evaluating the matrix element of the commutator with two molecular orbitals φ_i and φ_j, we obtain

$$\langle\varphi_i|[\vec{r}, H_{\rm M}]|\varphi_j\rangle = (\epsilon_j - \epsilon_i)\langle\varphi_i|\vec{r}|\varphi_j\rangle. \tag{7}$$

Combining Eqs. (6) and (7) yields

$$\langle\varphi_i|\vec{p}|\varphi_j\rangle = -\mathrm{i}\Omega_{ij}\langle\varphi_i|\vec{r}|\varphi_j\rangle, \tag{8}$$

where $\Omega_{ij} = \epsilon_j - \epsilon_i$. With Eq. (8), the expectation value of the momentum operator in Eq. (9) is eliminated to yield

$$H_{\rm el,ph} = \sum_i \epsilon_i b^{\dagger}_i b_i + \sum_{\vec{v}} \int d^3k\ \omega_{\vec{k}} a^{\dagger}_{\vec{k},\vec{v}} a_{\vec{k},\vec{v}} - \sum_{i,j,\vec{v}} \int d^3k\ C(\vec{k})\Omega_{ij}\vec{v}\cdot\vec{r}_{ij} b^{\dagger}_i b_j \left(a^{\dagger}_{\vec{k},\vec{v}} + a_{\vec{k},\vec{v}}\right). \tag{9}$$

The limit in which the photons can be described through a semiclassical approach is obtained[28] if the photon state is an eigenfunction of the destruction operator $a_{\vec{k},\vec{v}}$. This means that the photon degrees of freedom can be factorized. As a consequence, the electronic wave functions (e.g., the HOMO and the LUMO) are linearly combined in the resulting device wave function. Such a superposition is the expected behavior for a molecule coupled to a classical electromagnetic field.

C. Contacts

Finally, the left (L) and right (R) contact are added to the Hamiltonian $H_{\rm el,ph}$. We assume one-dimensional contacts whose states are labeled by the wave vector $\kappa_{\rm L(R)}$ in the left (right) contact, respectively. There are two types of additional terms that have to be added to Hamiltonian equation (9). The first one accounts for the energies of the contact states ($\epsilon_{\kappa_{\rm L(R)}}$),

$$H_{\rm L(R)} = \int d\kappa_{\rm L(R)}\ \epsilon_{\kappa_{\rm L(R)}} b^{\dagger}_{\kappa_{\rm L(R)}} b_{\kappa_{\rm L(R)}} \tag{10}$$

and the second term accounts for the coupling between the molecule and the contacts,

$$H_{\rm M,L(R)} = \sum_i \int d\kappa_{\rm L(R)} \times (\beta_{i,\kappa_{\rm L(R)}} b^{\dagger}_i b_{\kappa_{\rm L(R)}} + \beta^{*}_{\kappa_{\rm L(R)},i} b^{\dagger}_{\kappa_{\rm L(R)}} b_i). \tag{11}$$

The complete device Hamiltonian is then

$$H_{\rm device} = H_{\rm el,ph} + H_{\rm L} + H_{\rm R} + H_{\rm M,L} + H_{\rm M,R}. \tag{12}$$

While this operator appears to be rather cumbersome, in Sec. II D, we will show that a suitable choice of basis set leads to a fairly simple matrix representation.

D. Introduction of a finite tensor-product basis

In this section, the Hamiltonian of Eq. (12) is represented on a basis of selected functions which are tensor products of electron and photon states. The electron states are given in terms of the molecular orbitals (φ_i) by

$$|\varphi_i\rangle, \quad i = 1, 2, \ldots, N. \tag{13}$$

We limit the discussion to monochromatic light and the photon space that we consider is spanned by basis functions

Reuse of AIP Publishing content is subject to the terms: https://publishing.aip.org/authors/rights-and-permissions. Downloaded to IP: 147.173.66.125 On: Fri, 06 May 2016 07:53:59

with $n-1$ and n photons, respectively, of a given momentum $\vec{k}$ and polarization $\vec{v}$,

$$|(n-1)_{\vec{k},\vec{v}}\rangle,\ |n_{\vec{k},\vec{v}}\rangle. \tag{14}$$

This choice of basis functions is motivated by the sketch in Fig. 1. The outgoing state is one of $(n-1)_{\vec{k},\vec{v}}$ photons where the LUMO is coupled to the right contact. The quantized potential in Eq. (4) couples this state only to states with $n_{\vec{k},\vec{v}}$ and $(n-2)_{\vec{k},\vec{v}}$ photons. This is because this potential is assumed to be weak and higher orders of it (describing multiphoton transfers) are negligible. Similarly, the incoming photon state with $n_{\vec{k},\vec{v}}$ photons couples to $(n\pm 1)_{\vec{k},\vec{v}}$ ones. Combining these findings shows that processes describing electron transfer from the left to the right contact require the states in Eq. (14) and in the interest of simplicity, we limit the photon space through this minimal basis. The choice of the actual value of $n_{\vec{k},\vec{v}}$ specifies the strength of the coupling matrix between the electronic states (see Eq. (18)).

The basis of the combined electron-photon space is then given in terms of tensor products,

$$\begin{array}{c|ccc} & |\varphi_1\rangle & |\varphi_2\rangle & \dots\ |\varphi_N\rangle \\ \hline |(n-1)_{\vec{k},\vec{v}}\rangle & |\varphi_1\rangle\bigotimes|(n-1)_{\vec{k},\vec{v}}\rangle & |\varphi_2\rangle\bigotimes|(n-1)_{\vec{k},\vec{v}}\rangle & \dots\ |\varphi_N\rangle\bigotimes|(n-1)_{\vec{k},\vec{v}}\rangle \\ |n_{\vec{k},\vec{v}}\rangle & |\varphi_1\rangle\bigotimes|n_{\vec{k},\vec{v}}\rangle & |\varphi_2\rangle\bigotimes|n_{\vec{k},\vec{v}}\rangle & \dots\ |\varphi_N\rangle\bigotimes|n_{\vec{k},\vec{v}}\rangle \end{array}. \tag{15}$$

Similarly, the left and right contact states are combined with the photon states through a tensorial product,

$$\begin{array}{c|cc} & |\varphi_\kappa^{\mathrm{L}}\rangle & |\varphi_\kappa^{\mathrm{R}}\rangle \\ \hline |(n-1)_{\vec{k},\vec{v}}\rangle & |\varphi_\kappa^{\mathrm{L}}\rangle\bigotimes|(n-1)_{\vec{k},\vec{v}}\rangle & |\varphi_\kappa^{\mathrm{R}}\rangle\bigotimes|(n-1)_{\vec{k},\vec{v}}\rangle \\ |n_{\vec{k},\vec{v}}\rangle & |\varphi_\kappa^{\mathrm{L}}\rangle\bigotimes|n_{\vec{k},\vec{v}}\rangle & |\varphi_\kappa^{\mathrm{R}}\rangle\bigotimes|n_{\vec{k},\vec{v}}\rangle \end{array}. \tag{16}$$

The basis functions introduced in Eqs. (15) and (16) are then used to obtain a matrix representation of the second quantized Hamiltonian of Eq. (12),

$$\mathbf{H}_{\mathrm{device}} = \begin{pmatrix} \mathbf{H}_{\mathrm{L}} & \mathbf{M}_{\mathrm{L,M}} & & & & \\ \mathbf{M}_{\mathrm{L,M}}^{\dagger} & \mathbf{H}_{\mathrm{M}} & \mathbf{M}_{\mathrm{M,R}} & & \boldsymbol{\mu} & \\ & \mathbf{M}_{\mathrm{M,R}}^{\dagger} & \mathbf{H}_{\mathrm{R}} & & & \\ & & & \mathbf{H}_{\mathrm{L}}+\omega & \mathbf{M}_{\mathrm{L,M}} & \\ & \boldsymbol{\mu} & & \mathbf{M}_{\mathrm{L,M}}^{\dagger} & \mathbf{H}_{\mathrm{M}}+\omega & \mathbf{M}_{\mathrm{M,R}} \\ & & & & \mathbf{M}_{\mathrm{M,R}}^{\dagger} & \mathbf{H}_{\mathrm{R}}+\omega \end{pmatrix}. \tag{17}$$

In this representation, the sub-matrix $\mathbf{H}_{\mathrm{L(R)}}$ represents the left (right) contact. The blocks $\mathbf{M}_{\mathrm{L,M}}$ and $\mathbf{M}_{\mathrm{M,R}}$ describe the coupling of the molecule to the left (right) contact. $\mathbf{H}_{\mathrm{M}}$ is the Hückel matrix of the molecule and μ_{ij} is given by

$$\mu_{ij} = -C(\vec{k})\Omega_{ij}\vec{v}\cdot\vec{r}_{ij}\sqrt{n_{\vec{k},\vec{v}}}. \tag{18}$$

The energy shifts of the diagonal elements in Eq. (17) are obtained as follows. $H_{\mathrm{el,ph}}$ in Eq. (9) shows that the photons introduce energy shifts on the diagonal that are proportional to number of photons in the corresponding subspace. Since we can arbitrarily shift the energy, we choose it such that the photon energy of the $|(n-1)_{\vec{k},\vec{v}}\rangle$ state is zero. This explains why the subspace corresponding to $n_{\vec{k},\vec{v}}$ photons acquires a shift of ω. The subscript of ω has been dropped. As already mentioned, the photon number $n_{\vec{k},\vec{v}}$ also appears in the coupling matrix elements μ_{ij} (see Eq. (18)) and determines their magnitude.

Now we further simplify the matrix representation of Eq. (17). The boundary conditions that we employ stipulate that an electron arrives from the left contact and that the photon has not yet been absorbed. This means that the initial state is

$$|\varphi_{\mathrm{L}}\rangle\bigotimes|n_{\vec{k},\vec{v}}\rangle. \tag{19}$$

Similarly, on the right hand side, the outgoing state is

$$|\varphi_{\mathrm{R}}\rangle\bigotimes|(n-1)_{\vec{k},\vec{v}}\rangle. \tag{20}$$

We project the matrix in Eq. (17) onto the specified channels and re-order the basis functions to obtain a more intuitive representation

$$\mathbf{H}_{\mathrm{device}} = \begin{pmatrix} \mathbf{H}_{\mathrm{L}}+\omega & \mathbf{M}_{\mathrm{L,M}} & & \\ \mathbf{M}_{\mathrm{L,M}}^{\dagger} & \mathbf{H}_{\mathrm{M}}+\omega & \boldsymbol{\mu} & \\ & \boldsymbol{\mu} & \mathbf{H}_{\mathrm{M}} & \mathbf{M}_{\mathrm{M,R}} \\ & & \mathbf{M}_{\mathrm{M,R}}^{\dagger} & \mathbf{H}_{\mathrm{R}} \end{pmatrix}. \tag{21}$$

This Hamiltonian matrix describes a system with an electron arriving in the left contact while there are n photons of a given frequency and polarization. This state couples to one where a photon has been absorbed and the electron has been excited. The excited electron can then continue in the right contact.

Reuse of AIP Publishing content is subject to the terms: https://publishing.aip.org/authors/rights-and-permissions. Downloaded to IP: 147.173.66.125 On: Fri, 06 May 2016 07:53:59

III. ILLUSTRATIONS

A. Molecule coupled to photons

To illustrate the various aspects of the photocell model, we first consider a diatomic molecule. In the Hückel approximation, the diatomic is described by a two by two matrix,

$$\mathbf{H}_{\mathrm{M}} = \begin{pmatrix} 0 & t \\ t & 0 \end{pmatrix}, \tag{22}$$

where the diagonal elements are set to zero and the coupling matrix element between the atoms is given by t. The matrix $\boldsymbol{\mu}$ (Eq. (18)), describing the coupling between the photons and the electrons, is diagonal within the Hückel approximation,

$$\boldsymbol{\mu} = \begin{pmatrix} -\mu & 0 \\ 0 & \mu \end{pmatrix}. \tag{23}$$

This is because the operator $\vec{r}$ in Eq. (18) does not couple adjacent atoms. For simplicity, we assume $\vec{v} \| \vec{r}$, ignore the dependence of μ_{ij} on $\vec{k}$ and Ω_{ij} and treat it as a parameter. Using Eqs. (22) and (23), we combine the electronic and photon degrees of freedom to obtain

$$\mathbf{H}_{\mathrm{el,ph}} = \begin{pmatrix} \omega & t & -\mu & 0 \\ t & \omega & 0 & \mu \\ -\mu & 0 & 0 & t \\ 0 & \mu & t & 0 \end{pmatrix}. \tag{24}$$

This matrix describes the molecule coupled to a quantized photon field, it does not account for the contacts. We first examine the physical implications of $\mathbf{H}_{\mathrm{el,ph}}$. For the purpose of illustration, we arbitrarily set $t = -1$. Furthermore, for ω we choose a value of $\omega = 2|t|$, which means that the photon energy corresponds to the HOMO-LUMO gap and that the system is at resonance. The eigenvalues and eigenfunctions of $\mathbf{H}_{\mathrm{el,ph}}$ are given in Table I. We further assume that the electric field (and thus μ) is small. The first eigenvalue describes a state with an energy of $E \approx -1$, predominantly composed of the HOMO where the photon has been absorbed. Note that the first two coefficients of the eigenvectors correspond to the basis functions with n photons, whereas the third and fourth coefficients correspond to basis functions with $n-1$ photons. The fourth eigenvalue, with $E \approx 3$, corresponds to a wavefunction composed of the LUMO and n photons. The second and third eigenvalues are the interesting ones for the present purpose since they describe a resonance. At resonance, the HOMO and LUMO would be degenerate if not for the coupling between them provided by μ. As shown in Table I, the scalar $|\mu|$ is half the amount by which the two energy levels, resulting from the combination of HOMO and LUMO, are split. The associated eigenstates are superpositions of HOMO and LUMO, with n and $n-1$ photons, respectively.

TABLE I. Hückel eigenvalues and eigenvectors of a diatomic molecule coupled to a quantized photon field.

Eigenvalue	Eigenvector
$1-\sqrt{4+\mu^2}$	$\left(-\frac{2-\sqrt{4+\mu^2}}{\mu}, \frac{2-\sqrt{4+\mu^2}}{\mu}, 1, 1\right)$
$1-\mu$	$(-1,-1,-1,1)$
$1+\mu$	$(1,1,-1,1)$
$1+\sqrt{4+\mu^2}$	$\left(-\frac{2+\sqrt{4+\mu^2}}{\mu}, \frac{2+\sqrt{4+\mu^2}}{\mu}, 1, 1\right)$

B. Photovoltaic cell constructed from a diatomic molecule

The system consisting of the molecule coupled to the photons is now augmented by the contacts. The contacts are accounted for through a very simple version of the source-sink potentials.[13,14] In more detail, we employ a source (Σ_{L}) and a sink (Σ_{R}) potential that describe contacts in the wide band limit,[26]

$$\Sigma_{\mathrm{L}} = -\mathrm{i}\beta_{\mathrm{L}} \frac{1+r}{1-r} \tag{25}$$

and

$$\Sigma_{\mathrm{R}} = \mathrm{i}\beta_{\mathrm{R}}. \tag{26}$$

Σ_{L} and Σ_{R} are added to the diagonal element of the atoms the contacts are connected to, resulting in a model Hamiltonian $\mathbf{H}_{\mathrm{device}}$ for the total diatomic photocell,

$$\mathbf{H}_{\mathrm{device}} = \begin{pmatrix} \omega - \mathrm{i}\beta_{\mathrm{L}}\frac{1+r}{1-r} & t & -\mu & 0 \\ t & \omega & 0 & \mu \\ -\mu & 0 & 0 & t \\ 0 & \mu & t & \mathrm{i}\beta_{\mathrm{R}} \end{pmatrix}. \tag{27}$$

This matrix is then used to calculate the reflection coefficient $r(E,\omega)$ and thus the transmission probability $T(E,\omega) = 1 - |r(E,\omega)|^2$ of the photocell as a function of the energy E of the outgoing electron and as a function of the photon energy ω. For a given pair of E and ω, the reflection coefficient $r(E,\omega)$ can be simply obtained through solution of the equation

$$\det(\mathbf{H}_{\mathrm{device}}(r,\omega) - E) = 0. \tag{28}$$

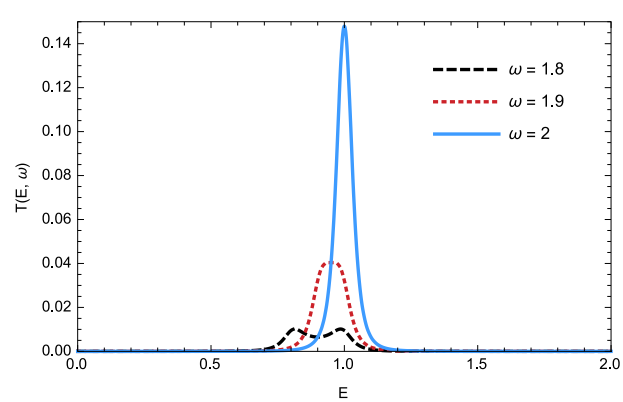

FIG. 2. Transmission probability ($T(E,\omega)$) of a photovoltaic cell constructed from a diatomic molecule. The transmission probability depends on the energy E of the outgoing electron and on ω, the energy of the photon involved. Values of ω varying around the resonance energy ($\omega_{\mathrm{res}} = 2$) are considered. The LUMO energy is 1 and this is where the resonance is observed on the E-axis. The coupling parameters for the contact-molecule interaction are $\beta_{\mathrm{L}} = \beta_{\mathrm{R}} = -0.1$ and $\mu = 0.01$.

Reuse of AIP Publishing content is subject to the terms: https://publishing.aip.org/authors/rights-and-permissions. Downloaded to IP: 147.173.66.125 On: Fri, 06 May 2016 07:53:59

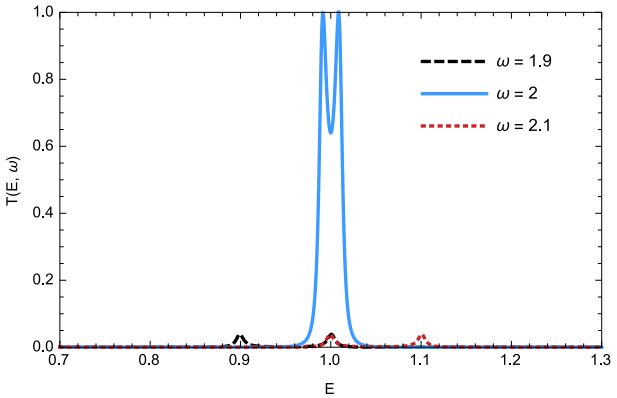

FIG. 3. Transmission probability ($T(E,\omega)$) of a photovoltaic constructed from a diatomic molecule weakly coupled to the external contacts. The weak coupling gives rise to two sharp resonances that are separated by $2|\mu|$. The coupling parameters for the contact-molecule interaction are $\beta_L = \beta_R = -0.01$ and $\mu = 0.01$.

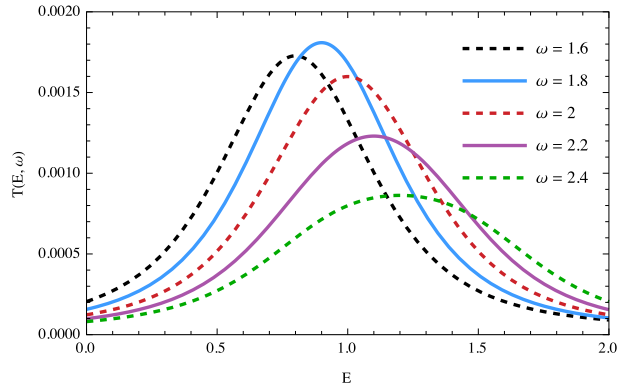

FIG. 4. Transmission probability ($T(E,\omega)$) of a photovoltaic cell constructed from a diatomic molecule strongly coupled to the contacts. Broad resonances of weak transmission probability are observed. The coupling parameters for the contact-molecule interaction are $\beta_L = \beta_R = -1$ and $\mu = 0.01$.

In Fig. 2, $T(E,\omega)$ is plotted for the photocell constructed from the diatomic molecule. The photon energy is varied as indicated in the figure, resulting in a family of curves. At resonance ($\omega = 2|t|$), there is a single peak that splits into two when the photon energy deviates from the resonance condition. The resulting two peaks separate more and more and the peak height decreases rapidly with increasing $|\omega - \omega_{res}|$. The two peaks originate of course from the HOMO and LUMO. Inspection of Eq. (21) shows that the HOMO contribution to the device wave function is raised by the energy of the photon, whereas the LUMO contribution remains at its position upon variation of the ω. Next we reduce the coupling of the molecule to the contacts by a factor of 10, i.e., $\beta_L = \beta_R = -0.01$. The corresponding $T(E,\omega)$ is shown in Fig. 3. The graphs reveal a number of interesting features. First there are two maxima visible that obviously originate from the two molecular levels. The splitting between the levels is given by twice the coupling element $|\mu|$. In a time-dependent approach, this splitting equals the Rabi frequency[7] which determines how fast the system oscillates between the HOMO and LUMO. Clearly, the split resonance in Fig. 3 is related to the two resonant eigenstates with energies $E = 1 \pm \mu$, listed in Table I. Another very interesting aspect of the weak-coupling case is that the photo-induced transmission probability reaches the maximum possible value of one. This is a characteristic of the weak coupling limit in which the molecule represents a Fabry-Pérot resonator that is completely transparent for electrons with a wavelength corresponding to the LUMO energy plus or minus μ.

Next we discuss the case where the molecule is strongly coupled ($\beta_L = \beta_R = t$) to the contacts. As can be seen in Fig. 4, broad maxima appear in which the Rabi splitting is not visible anymore. The maximum is shifted down or up in energy depending on whether the photon energy is slightly below or above the resonance frequency, respectively. Furthermore, the height of the resonances is reduced by three orders of magnitude compared to the weak coupling case. Note that the maximum value of $T(E,\omega)$ is not obtained for $\omega = \omega_{res}$. This is a consequence of the strong coupling to the contacts.

Finally, we discuss the dependence of the transmission probability on μ. This dependence can be extracted analytically for the photocell built with the diatomic molecule. Using the *Mathematica* program to perform the algebra, we find that T depends quadratically on μ. According to Eq. (18), μ^2 is proportional the number of photons, i.e., to the energy density of the field. This is the expected result.

C. Photovoltaic cell constructed from the azulene molecule

Now we investigate a photovoltaic cell constructed with the azulene molecule. Azulene is a blue colored compound whose chemical structure is shown in Fig. 5. It is suitable for the construction of conventional photovoltaic cells because of its absorption spectrum in the visible range. Since azulene does not exhibit spherical symmetry, the orientation of the electric field is a factor that influences the transmission probability. Azulene has C_{2v} symmetry and the HOMO and LUMO are antisymmetric or symmetric with respect to the molecular axis, respectively. We focus on ω values corresponding to the HOMO-LUMO gap, i.e., we consider the system at resonance. The left contact is attached to atom number 4 and the right contact to atom 10. Also in this case, we set $t = -1$. To calculate μ_{ij} of Eq. (18), we equate all the bond lengths and scale them so that they have a

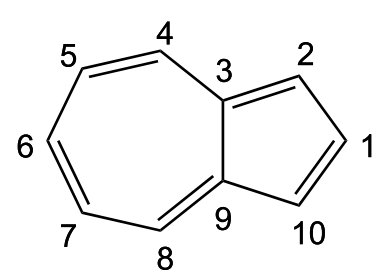

FIG. 5. Molecular structure of azulene with the numbering scheme superimposed. We refer to the C_2 axis as the molecular axis.

Reuse of AIP Publishing content is subject to the terms: https://publishing.aip.org/authors/rights-and-permissions. Downloaded to IP: 147.173.66.125 On: Fri, 06 May 2016 07:53:59

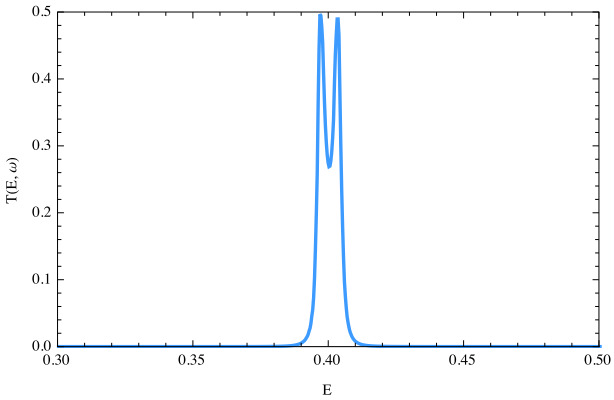

FIG. 6. Transmission probability ($T(E,\omega)$) of a photovoltaic cell constructed from an azulene molecule. The ω value considered corresponds to the resonance energy ($\omega_{\text{res}} \approx 0.878$). The applied electric field is oriented perpendicular to the molecular axis and the left and right contact are in the 4 and 10 position, respectively. A split resonance is obtained which arises from the interaction of the HOMO and LUMO resulting in two admixtures that are separated in energy because they are coupled through the photons. The resonance appears at 0.4 on the energy axis which corresponds to the LUMO energy of azulene.

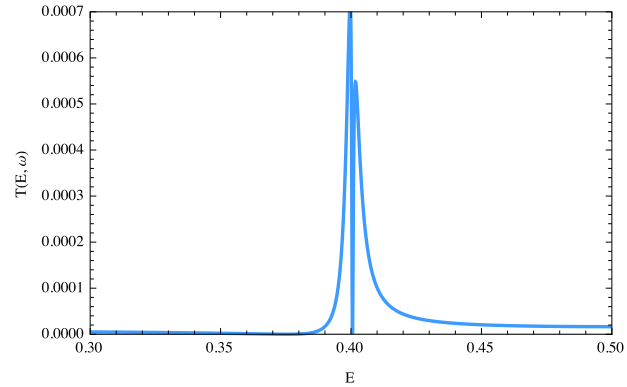

FIG. 8. Transmission probability ($T(E,\omega)$) of a photovoltaic cell constructed from an azulene molecule. The ω value considered corresponds to the resonance energy ($\omega_{\text{res}} \approx 0.878$). The electric field is oriented along the molecular axis and the left and right contacts are in positions 4 and 10, respectively. Overall a very small transmission probability is obtained that vanishes exactly at $E = E_{\text{LUMO}}$, where E_{LUMO} is the energy of the LUMO of azulene.

value of 1. The corresponding additional scaling factor a in Eq. (18) is then absorbed together with other factors in the parameter μ, i.e., $\mu_{ij} = -aC(\vec{k})\Omega_{ij}\vec{v} \cdot \vec{r}_{ij}\sqrt{n_{\vec{k},\vec{v}}} = \mu\, \vec{v} \cdot \vec{r}_{ij}$. Furthermore, for the contact-molecule interaction, we employ $\beta_{\text{L}} = \beta_{\text{R}} = -0.1$. In Fig. 6, $T(E,\omega_{\text{res}})$ is shown for an electric field perpendicular to the molecular axis. In this case the electric field couples the HOMO to the LUMO and consequently, a resonance in the transmission profile is observed. As in the case of the diatomic molecule with weak coupling to the contacts, the resonance peak is split in two.

To further illustrate our model for coherent molecular photocells, we analyze the device wave function. In particular, we focus on the molecular part of the wave function and note that there are two such components since device Hamiltonian equation (21) is a direct sum with two molecular Hamiltonian matrices. One of these matrices describes a system where the photon has not yet been absorbed and the other one a system where it has been absorbed. We focus on $\omega = \omega_{\text{res}}$ and choose E such that it corresponds to the first maximum of $T(E,\omega_{\text{res}})$ in Fig. 6. In Fig. 7, we show the two molecular components of the device wave function which correspond to $n_{\vec{k},\vec{v}}$ and $(n-1)_{\vec{k},\vec{v}}$ photons. The component in the left panel resembles the HOMO, whereas the component in the right panel resembles the LUMO. This is the expected structure of the device wave function at resonance. Furthermore, since this function describes electron transport, it is complex valued. In the left panel of Fig. 7, the complex part is very small and invisible on the scale of the plot. In the right panel, small black and white disks are visible around the atoms and they represent the imaginary part of the wave function while the blue and red disks represent the real part.

For an electric field oriented along the molecular axis (Fig. 8), overall $T(E,\omega_{\text{res}})$ is very small. If the molecule were isolated from the contacts, such a field would not couple the HOMO to the LUMO at all. However, the presence of the contacts reduces the symmetry and yields a non-zero $T(E,\omega_{\text{res}})$. Interestingly, if the energy of the outgoing electron

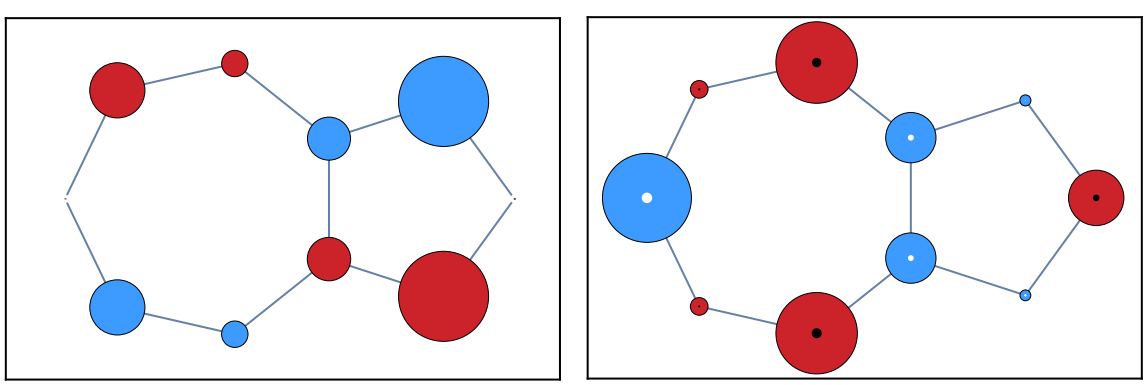

FIG. 7. The molecular components of the device wave function of the first resonance in Fig. 6 ($\omega = \omega_{\text{res}}$ and $E = 0.397$). The first panel shows the component of the wave function with an extra photon and the second panel shows the component where the photon has been absorbed. While the first component resembles the HOMO, the second one resembles the LUMO. The blue and red disks represent the positive and negative real parts of the orbital coefficients, respectively. The radii are proportional to the absolute values of the coefficients. Analogously, the white and black disks represent the imaginary parts of the orbital coefficients.

Reuse of AIP Publishing content is subject to the terms: https://publishing.aip.org/authors/rights-and-permissions. Downloaded to IP: 147.173.66.125 On: Fri, 06 May 2016 07:53:59

is equal to the LUMO energy, the transmission probability vanishes entirely.

IV. CONCLUSION

We provide a theory for a coherent molecular photocell that is reduced to the essential elements of such a device. The model accounts for the contacts, the molecule, and the photons. Each of these components and the interactions between them are described through as simple a means as possible, resulting in a transparent formalism. To illustrate the developed model, we focus on generic examples and show how photon absorption can lead to significant transmission probabilities that would otherwise vanish. The passage of the electron through the molecule is accompanied by an increase in the electronic energy and a decrease of the number of photons. In the examples considered, several phenomena such as Rabi oscillations and Fabry-Pérot resonances are observed that are to be expected based on earlier studies using a semiclassical approach.[8–10] We also show that the transmission probability depends on the photon polarization. While we employ somewhat arbitrary parameters in the illustrations, the model should nonetheless provide useful approximate descriptions. As in our work on molecular electronics (see, e.g., Refs. 13, 14, 18, and 19), we focus on qualitative aspects that are largely independent of the actual values of the parameters in the model.

In future work, we will explore various improvements and extensions of the simple model presented here. For instance, through the addition of a suitable sink potential,[26] additional electron channels can be added that account for the conduction band of the left contact. Furthermore, the method developed here within the Hückel approximation can be extended to other effective one-particle pictures. For example, it should be possible to employ Hartree-Fock theory to provide the required orbitals.

ACKNOWLEDGMENTS

M.E. and M.-A.B. would like to acknowledge the financial support provided by NSERC.

[1]M. Grätzel, Acc. Chem. Res. **42**, 1788 (2009).
[2]M. Galperin and A. Nitzan, Phys. Rev. Lett. **95**, 206802 (2005).
[3]M. Galperin and A. Nitzan, J. Chem. Phys. **124**, 234709 (2006).
[4]M. Galperin and A. Nitzan, Phys. Chem. Chem. Phys. **14**, 9421 (2012).
[5]S. Ajisaka, B. Zunkovic, and Y. Dubi, Sci. Rep. **5**, 8312 (2015).
[6]J. Jackson, *Classical Electrodynamics* (Wiley, 1975).
[7]C. Cohen-Tannoudji, B. Diu, and F. Laloë, *Quantum Mechanics* (Wiley, 1977), Vols. I and II.
[8]R. Volkovich and U. Peskin, Phys. Rev. B **83**, 033403 (2011).
[9]U. Peskin and M. Galperin, J. Chem. Phys. **136**, 044107 (2012).
[10]A. J. White, U. Peskin, and M. Galperin, Phys. Rev. B **88**, 205424 (2013).
[11]Y. Selzer and U. Peskin, J. Phys. Chem. C **117**, 22369 (2013).
[12]M. A. Ochoa, Y. Selzer, U. Peskin, and M. Galperin, J. Phys. Chem. Lett. **6**, 470 (2015).
[13]F. Goyer, M. Ernzerhof, and M. Zhuang, J. Chem. Phys. **126**, 144104 (2007).
[14]M. Ernzerhof, J. Chem. Phys. **127**, 204709 (2007).
[15]B. Pickup and P. Fowler, Chem. Phys. Lett. **459**, 198 (2008).
[16]M. Ratner, Nat. Nanotechnol. **8**, 378 (2013).
[17]S. Battacharyya, A. Kibel, G. Kodis, P. A. Liddell, M. Gervaldo, D. Gust, and S. Lindsay, Nano Lett. **11**, 2709 (2011).
[18]M. Ernzerhof, M. Zhuang, and P. Rocheleau, J. Chem. Phys. **123**, 134704 (2005).
[19]D. Mayou, Y. Zhou, and M. Ernzerhof, J. Phys. Chem. C **117**, 7870 (2013).
[20]C. M. Guedon, H. Valkenier, T. Markussen, K. S. Thygesen, J. C. Hummelen, and S. J. van der Molen, Nat. Nanotechnol. **7**, 305 (2012).
[21]H. Valkenier, C. M. Guedon, T. Markussen, K. S. Thygesen, S. J. van der Molen, and J. C. Hummelen, Phys. Chem. Chem. Phys. **16**, 653 (2014).
[22]D. Z. Manrique, C. Huang, M. Baghernejad, X. Zhao, O. A. Al-Owaedi, H. Sadeghi, V. Kaliginedi, W. Hong, M. Gulcur, T. Wandlowski, M. R. Bryce, and C. J. Lambert, Nat. Commun. **6**, 6389 (2015).
[23]P. Brumer and M. Shapiro, *Principles and Applications of the Quantum Control of Molecular Processes* (Wiley Interscience, 2003).
[24]M. Kilgour and D. Segal, J. Chem. Phys. **143**, 024111 (2015).
[25]K. Haule and J. Bonča, Phys. Rev. B **59**, 13087 (1999).
[26]M. Ernzerhof, J. Chem. Phys. **140**, 114708 (2014).
[27]C. Aslangul, *Mécanique Quantique 2* (De Boeck, 2015).
[28]C. Cohen-Tannoudji, J. Dupont-Roc, and G. Grynberg, *Photons and Atoms: Introduction to Quantum Electrodynamics* (Wiley-VCH Verlag GmbH, 1989).

Reuse of AIP Publishing content is subject to the terms: https://publishing.aip.org/authors/rights-and-permissions. Downloaded to IP: 147.173.66.125 On: Fri, 06 May 2016 07:53:59